JPEG Reversible Data Hiding via Effective 2D Mappings Using Dual-Basis Offset Adjustment

Qi Chang [1], Lukai Zhang [1], Ye Yao [1], Mengyao Xiao [2], Haorui Wu [3*]

[1]Hangzhou Dianzi University, Hangzhou, China, [2]Nanchang University, Nanchang, China, [3]University of International Relations, Beijing, China

Introduction

Reversible data hiding (RDH) in JPEG images enables embedding secret data with exact content recovery. Schemes with a higher peak signal-to-noise ratio (PSNR) and a lower file size increase (FSI) at the same embedding capacity (EC) are preferred. RDH is widely applied in areas such as copyright authentication and privacy preservation.

We propose a JPEG RDH technique based on two-dimensional (2D) mapping generation and modification, incorporating an offset adjustment strategy from dual-basis types to effectively exploit both peak and non-peak coefficients of non-zero bins of alternating current (AC) coefficients histograms (ACHs) simultaneously.

Experiments demonstrate that the proposed method outperforms several state-of-the-art approaches in terms of visual quality and file size changes.

Proposed Method

Firstly, numerous 2D mappings are generated through a two-stage process. In the first stage, a diverse set of derived mappings is designed by locally fine-tuning two basis types of 2D mappings. For the first basis type mapping, mainstream 2D mappings primarily focus on expanding coefficient pairs with low absolute values, which are typically concentrated in the high-frequency bins of 2D ACH. The classic shape of this form is illustrated in Fig. 1(a). Moreover, for the second basis type mapping, closely situated coefficients often exhibit correlation, which is directly reflected along the diagonal of 2D ACH of paired coefficient values. To address this, a second form of basis mapping is designed as shown in Fig. 1(c).

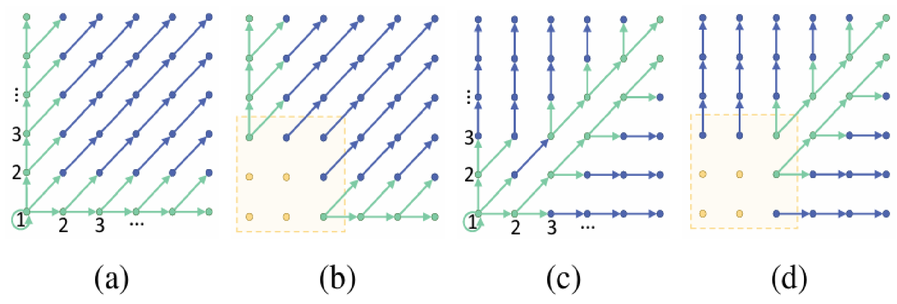

Fig. 1: (a) A mapping expands low absolute value bins. (b) Type I. (c) A mapping expands diagonal bins. (d) Type II.

In the second stage, candidate mappings are further created by applying offset adjustments to the derived mappings, optimizing the utilization of both peak and non-peak coefficients. Specifically, Fig. 2 illustrates the offset adjustment process using one mapping of Type I as an example.

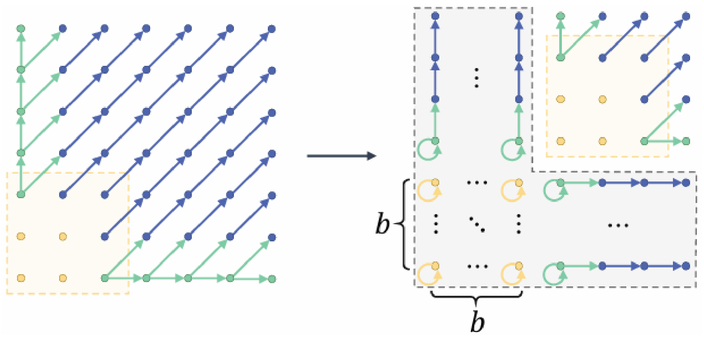

Fig. 2: The illustration of offset adjustment strategy from a derived Type I mapping to a candidate mapping.

Secondly, a few effective alternative mappings are selected from the above candidates by evaluating the embedding results of extensive actual implementations through a rate-distortion optimization model. Finally, alternative mappings are utilized to adaptively modify 2D ACHs, accounting for the diversity of image content.

Related Works

Existing JPEG RDH methods fall into three main categories: modifying the quantization table, modifying the Huffman table and modifying quantized discrete cosine transform (DCT) coefficients. Among these, quantized DCT coefficients modification is the most pivotal and extensively studied.

A representative early work by Huang *et al.* [1] extended one-dimensional (1D) histogram shifting to the DCT domain by embedding data into quantized AC coefficients with values ± 1, while preserving direct current (DC) and zero-valued AC coefficients to reduce FSI. Following [1], subsequent studies further explored the embedding of ± 1 by optimizing coefficient selection to improve histogram construction, e.g., He *et al.* [2] introduced a negative influence measure. Later, Xiao *et al.* [3] extended embedding beyond ± 1, and Li *et al.* [4] proposed 2D histograms modification, inspiring further improvements based on coefficient pairing and refined 2D mapping generation. For example, Li *et al.* [5] designed progressive histogram modification.

Experimental Results

We compare the proposed scheme with those of He *et al.* [2], Xiao *et al.* [3], Li *et al.* [4] and Li *et al.* [5], using the USC-SIPI and Kodak databases.The performance is evaluated in terms of PSNR and FSI.

TABLE I: Comparison of PSNR (dB) and FSI (bits).

Databases	Images	Methods	PSNR							FSI						
			QF=70		QF=80		QF=90		Average	QF=70		QF=80		QF=90		Average
			7,000	15,000	7,000	15,000	7,000	15,000		7,000	15,000	7,000	15,000	7,000	15,000	
USC-SIPI	Baboon	Proposed	**44.25**	**38.75**	**46.19**	**40.58**	**48.99**	43.56	**43.72**	**6,560**	**17,048**	**7,136**	**17,224**	**7,992**	**17,656**	**12,269**
		He *et al.* [2]	43.97	38.65	45.88	40.43	48.56	43.47	43.49	9,632	22,592	9,408	22,120	10,712	24,624	16,515
		Xiao *et al.* [3]	43.84	38.56	45.73	40.30	48.53	43.14	43.35	7,816	18,944	7,800	18,776	9,784	20,072	13,865
		Li *et al.* [4]	44.00	38.36	45.92	40.40	48.67	43.54	43.48	8,608	19,760	8,672	19,976	10,104	22,352	14,912
		Li *et al.* [5]	44.20	38.36	45.99	40.27	48.85	**43.65**	43.56	6,736	17,440	7,864	17,760	8,720	18,432	12,795
	Barbara	Proposed	**45.80**	39.26	**48.79**	42.40	**53.35**	**47.88**	**46.25**	**6,536**	**16,680**	6,664	**16,072**	**6,704**	**16,296**	**11,492**
		He *et al.* [2]	45.47	39.61	48.67	42.44	53.13	47.71	46.17	9,272	22,544	8,872	21,752	9,512	21,904	15,643
		Xiao *et al.* [3]	45.51	**39.63**	48.68	**42.45**	53.05	47.69	46.17	7,016	19,408	7,424	17,224	7,136	18,128	12,723
		Li *et al.* [4]	44.99	38.78	48.23	41.69	52.80	47.09	45.60	8,152	19,920	7,888	20,624	9,040	20,424	14,341
		Li *et al.* [5]	44.92	38.88	48.50	41.67	53.21	46.77	45.66	6,960	17,920	**6,416**	17,984	6,912	18,808	12,500
Kodak	Kodim06	Proposed	**47.64**	**42.73**	**50.18**	**45.09**	**55.10**	**49.10**	**48.31**	**6,104**	**14,616**	**6,736**	**16,272**	**6,312**	**16,288**	**11,055**
		He *et al.* [2]	47.28	42.36	49.70	44.66	54.90	48.85	47.96	7,736	19,696	9,176	21,016	9,952	24,240	15,303
		Xiao *et al.* [3]	47.32	42.44	49.88	44.83	54.80	48.82	48.02	7,056	16,448	7,576	17,888	7,672	18,216	12,476
		Li *et al.* [4]	46.76	42.09	49.35	44.34	54.47	48.27	47.55	7,512	18,496	8,360	20,296	8,448	24,280	14,565
		Li *et al.* [5]	47.36	42.24	49.71	44.38	54.36	48.35	47.73	6,208	15,816	7,072	18,008	6,696	18,776	12,096
	Kodim16	Proposed	**48.34**	**43.63**	**51.12**	**46.18**	**55.98**	**50.98**	**49.37**	6,256	**14,088**	6,632	**15,680**	**7,132**	**16,824**	**11,102**
		He *et al.* [2]	47.97	43.19	50.64	45.77	55.92	50.70	49.03	8,224	20,688	9,472	20,408	10,064	22,176	15,172
		Xiao *et al.* [3]	48.15	43.29	50.80	45.86	55.83	50.78	49.12	6,920	15,704	7,168	15,872	7,928	17,880	11,912
		Li *et al.* [4]	47.72	43.06	50.37	45.55	55.55	50.16	48.74	7,904	18,960	8,496	19,304	9,328	21,144	14,189
		Li *et al.* [5]	47.98	43.06	50.65	45.50	55.65	50.14	48.83	**6,032**	15,856	**6,456**	15,920	7,192	17,200	11,443

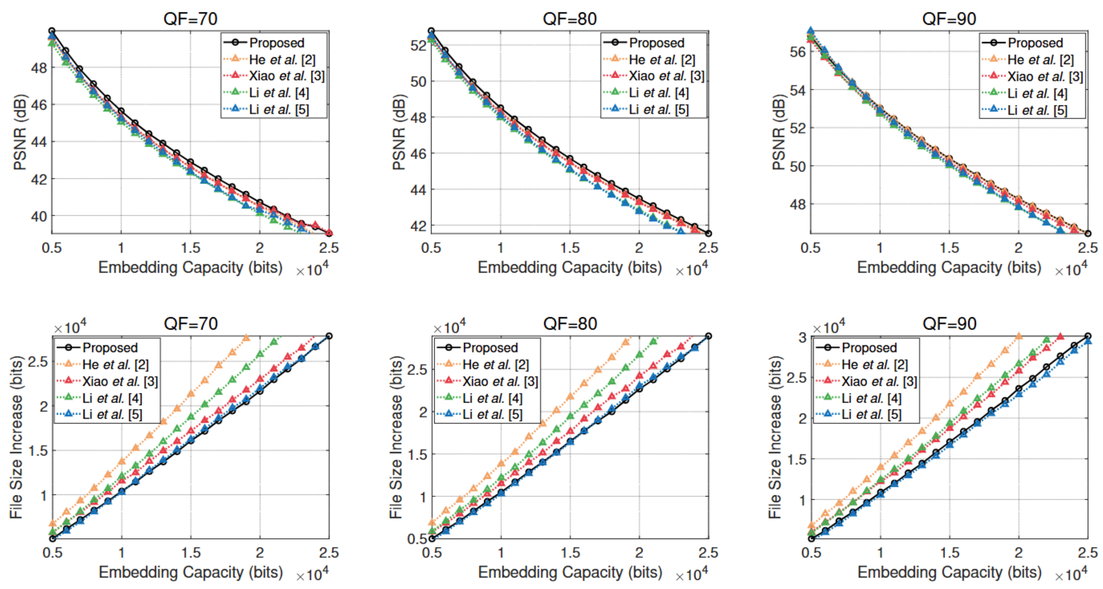

Fig. 3: Comparisons of average PSNR (dB) and FSI (bits) for all 24 images from Kodak database.

References

[1] F. Huang *et al.*, "Reversible data hiding in JPEG images," TCSVT, vol. 26, no. 9,pp. 1610-1621, 2016.
[2] J. He *et al*, "Reversible data hiding in JPEG images based on negative influence models," TIFS,vol. 15, pp. 2121-2133, 2020.
[3] M. Xiao *et al*, "Efficient reversible data hiding for JPEG images with multiple histograms modification," TCSVT, vol. 31, no. 7, pp. 2535-2546, 2021.
[4] N. Li *et al*, "Reversible data hiding for JPEG images based on pairwise nonzero AC coefficient expansion," SP, vol. 171,p. 107476, 2020.
[5] F. Li *et al*, "Progressive histogram modification for JPEG reversible data hiding," TCSVT, vol. 34, no. 2, pp. 1241-1254, 2024.